

RESEARCH ARTICLE

Open Access



# Identifying global expression patterns and key regulators in epithelial to mesenchymal transition through multi-study integration

Princy Parsana<sup>1</sup>, Sarah R. Amend<sup>2</sup>, James Hernandez<sup>2</sup>, Kenneth J. Pienta<sup>2</sup> and Alexis Battle<sup>1\*</sup>

## Abstract

**Background:** Epithelial to mesenchymal transition (EMT) is the process by which stationary epithelial cells transdifferentiate to mesenchymal cells with increased motility. EMT is integral in early stages of development and wound healing. Studies have shown that EMT could be a critical early event in tumor metastasis that is involved in acquisition of migratory and invasive properties in multiple carcinomas.

**Methods:** In this study, we used 15 published gene expression microarray datasets from Gene Expression Omnibus (GEO) that represent 12 cell lines from 6 cancer types across 95 observations (45 unique samples and 50 replicates) with different modes of induction of EMT or the reverse transition, mesenchymal to epithelial transition (MET). We integrated multiple gene expression datasets while considering study differences, batch effects, and noise in gene expression measurements. A universal differential EMT gene list was obtained by normalizing and correcting the data using four approaches, computing differential expression from each, and identifying a consensus ranking. We confirmed our discovery of novel EMT genes at mRNA and protein levels in an in vitro EMT model of prostate cancer – PC3 epi, EMT and Taxol resistant cell lines. We validate our discovery of *C1orf116* as a novel EMT regulator by siRNA knockdown of *C1orf116* in PC3 epithelial cells.

**Results:** Among differentially expressed genes, we found known epithelial and mesenchymal marker genes such as *CDH1* and *ZEB1*. Additionally, we discovered genes known in a subset of carcinomas that were unknown in prostate cancer. This included epithelial specific *LSR* and *S100A14* and mesenchymal specific *DPYSL3*. Furthermore, we also discovered novel EMT genes including a poorly-characterized gene *C1orf116*. We show that decreased expression of *C1orf116* is associated with poor prognosis in lung and prostate cancer patients. We demonstrate that knockdown of *C1orf116* expression induced expression of mesenchymal genes in epithelial prostate cancer cell line PC3-epi cells, suggesting it as a candidate driver of the epithelial phenotype.

**Conclusions:** This comprehensive approach of statistical analysis and functional validation identified global expression patterns in EMT and candidate regulatory genes, thereby both extending current knowledge and identifying novel drivers of EMT.

**Keywords:** EMT, Metastasis, Prostate cancer, C1orf116, Multi-study integration

\* Correspondence: [ajbattle@cs.jhu.edu](mailto:ajbattle@cs.jhu.edu)

<sup>1</sup>Department of Computer Science, Johns Hopkins University, Baltimore, MD 21218, USA

Full list of author information is available at the end of the article



## Background

Cancer is the second leading cause of death in United States. Metastasis is the leading cause of cancer-related morbidity and mortality [1], but identifying tumors with metastatic potential remains a challenge [2]. Tumor metastasis is a multi-step process in which primary tumor cells disseminate from their site of origin to seed secondary tumors at a distant site [3]. It is believed that in a critical early event in cancer progression, metastatic cancer cells undergo an epithelial to mesenchymal transition (EMT). During EMT, stationary epithelial cells lose cell polarity and transdifferentiate to spindle-shaped motile mesenchymal cells. EMT is a crucial physiologic process involved in early development during embryogenesis and organogenesis. It also plays an important role in tissue regeneration and wound healing. However, in cancer EMT may contribute to tumor progression and malignant transformation. Several epithelial cancer cells have been described to undergo EMT transform to a more malignant phenotype [4] that can further promote formation of secondary tumors [5].

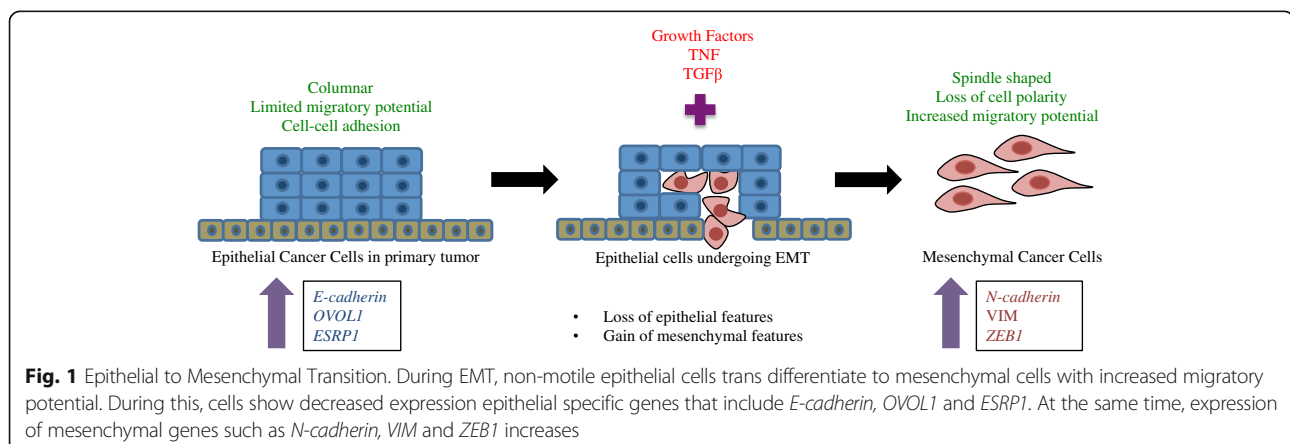
The role of EMT has been frequently debated in clinical cancer metastasis [6]. However, several in vitro studies have shown that epithelial cancer cells can undergo EMT in response to a combination of signals from the tumor microenvironment [2]. During EMT, cells go through multiple morphological and biochemical changes resulting in loss of epithelial properties coupled with gain of mesenchymal characteristics [7–21]. Microarrays have been widely used to study gene expression patterns of cell populations under different experimental settings, including EMT-inducing conditions (Fig. 1). While there have been many studies investigating the effect of a gene or pathway in EMT, none have explored the universal changes across multiple cancer tissue types or EMT induction methods.

Several gene expression datasets examining EMT in a variety of different cell lines under different conditions

are available on open access databases such as Gene Expression Omnibus (GEO) [22]. It has been demonstrated that re-use and aggregation of public gene expression data facilitates discovery of signals too weak to be detected in an individual experiment [23–26]. Gröger et al. performed meta-analysis of 18 EMT gene expression studies and identified 130 core-EMT genes, which were differentially expressed in at least 10 of the 18 studies [27]. Genes such as *TGFB*, *GNG11*, *TIMP1*, *ETS1*, *S100A14*, *DPYSL3* and *C1orf116* that we discovered as differential EMT, were not found in their core EMT gene list. Furthermore, we experimentally validated some of these genes (*S100A14*, *DPYSL3* and *C1orf116*) in PC3 epithelial, PC3-EMT and PC3-taxol resistant cell lines confirming their association in EMT. Also, each dataset in [27] was confined by small sample size per class ( $n < =6$ ). The drawback with underpowered studies are: a) low probability of identifying true effects b) overestimation of effect size [28, 29]. Therefore, genes that showed consistent moderate effects across datasets could be missed. In contrast, systematic integration of multiple studies promotes reliable detection of consistent gene expression changes that may otherwise be false negatives in results obtained from individual experiment [30]. At the same time, it helps avoid false discoveries that could result from intra-study variability resulting from single experiment.

Batch effects and noise introduce spurious signal and correlations in microarray gene expression data [31, 32]. Therefore, data normalization is crucial in order to correct the data for unwanted biological or non-biological effects. However, Groger et al. do not account for batch effects, cross-platform differences, or cross-tissue effects in their meta-analyses study that could potentially lead to false positive findings.

In this study, to identify universal EMT genes common across multiple cancer types, we integrated 15 independent gene expression studies representing 12 cell lines (49



epithelial and 46 mesenchymal phenotypes) from 6 cancer tissue types and multiple EMT induction modalities (Table 1, Additional file 1: Table S1). After correcting data to account for cross-study differences, cross-platform differences, and other sources of noise, we performed differential expression analysis and identified global changes in gene expression patterns between epithelial and mesenchymal states (Fig. 2). Importantly, our candidate gene list was enriched for EMT-related genes and we identified known markers of EMT. In addition, we also identified EMT genes that had only been described in a sub-set of malignant disease states, but were previously unknown in prostate cancer (e.g. *LSR*, *S11A14*, *DPYSL3*), implying a common EMT program across multiple cancer types. We further identified genes that had not been previously characterized in EMT in any disease state including *C1orf116*, which we then experimentally validated using siRNA knockdown in PC3 epithelial cells. This approach of multi-study integration enabled identification of differential EMT genes universal across different types of cancer. Functional validations of these genes indicate manifestation of molecular mechanisms contributing to EMT shared across disease types. This study also identifies an uncharacterized candidate novel EMT regulator gene *C1orf116*. These findings thereby extend our knowledge and understanding of EMT biology.

## Methods

### Data overview

We used 15 published EMT microarray gene expression datasets from GEO (Gene Expression Omnibus) (Table 1, Additional file 1: Table S1). This comprises of 95

observations (45 unique samples and 50 replicates), 49 epithelial and 46 mesenchymal cell lines exposed to different treatment modalities. The cell lines come from 6 different tissue types including breast, prostate, colon, esophageal, liver and retinal pigment and 4 different microarray platforms (8 chips), Affymetrix, Agilent, Stanford Microarray Database (SMD) and Illumina. All the datasets were downloaded in the format they were submitted to GEO. We mapped platform specific probe IDs to Ensembl IDs and gene symbols. When multiple probes mapped to same gene, we used median values to represent expression of that gene. We used 7276 genes common across all datasets.

### Data normalization

This work combined data from multiple studies spanning diverse cell lines and different platforms. Batch effects and noise are inherent in gene expression data. To account for confounders in data as a result of cross-study and cross-platform effects, we used multiple correction methods, such as quantile normalization (QN), Surrogate Variable Analysis (SVA), Quantile normalization followed by SVA and Column Standardized Median Centered (MCtr). We merged all 15 datasets into one matrix prior to quantile normalization and SVA. For CMSC, we individually processed each study and combined them after normalization.

### Quantile normalization

Quantile normalization makes the gene expression distribution of each sample in the dataset the same. Given a dataset  $D$ , with 'g' genes and 'n' samples:

**Table 1** Dataset information

GEO ID	Platform ID	Disease Type	Cell line	Samples*	Ref
GSE12811	GPL7319	Breast	MCF10A	3	[7]
GSE13915	GPL7785	Breast	BT549, EFM19	4	[8]
GSE18070	GPL570	Breast	MCF10CA1h	9	[9]
GSE28569	GPL6480	Breast	MCF10A	8	[10]
GSE39356	GPL6480	Breast	MCF-7	4	[11]
GSE8240	GPL3921	Breast	MCF10A	11	[12]
GSE12203	GPL2700	Colon	Caco-2	4	[13]
GSE14773	GPL570	Colon	HT29, SW480	8	[14]
GSE27424	GPL570	Esophageal	EPc2-hTERT	12	[15]
GSE26391	GPL6244	Liver	HCC-1.1, HCC-1.2	8	[16]
GSE14405	GPL570	Prostate	PC3, TEM4, TEM2	6	[17]
GSE22010	GPL6244	Prostate	PrEC-hTERT	2	[18]
GSE22764	GPL6884	Prostate	PC3	6	[19]
GSE43489	GPL570	Prostate	PC3	4	[20]
GSE12548	GPL570	Retinal pigment	ARPE19	6	[21]

\*Indicates the number of samples included in our study

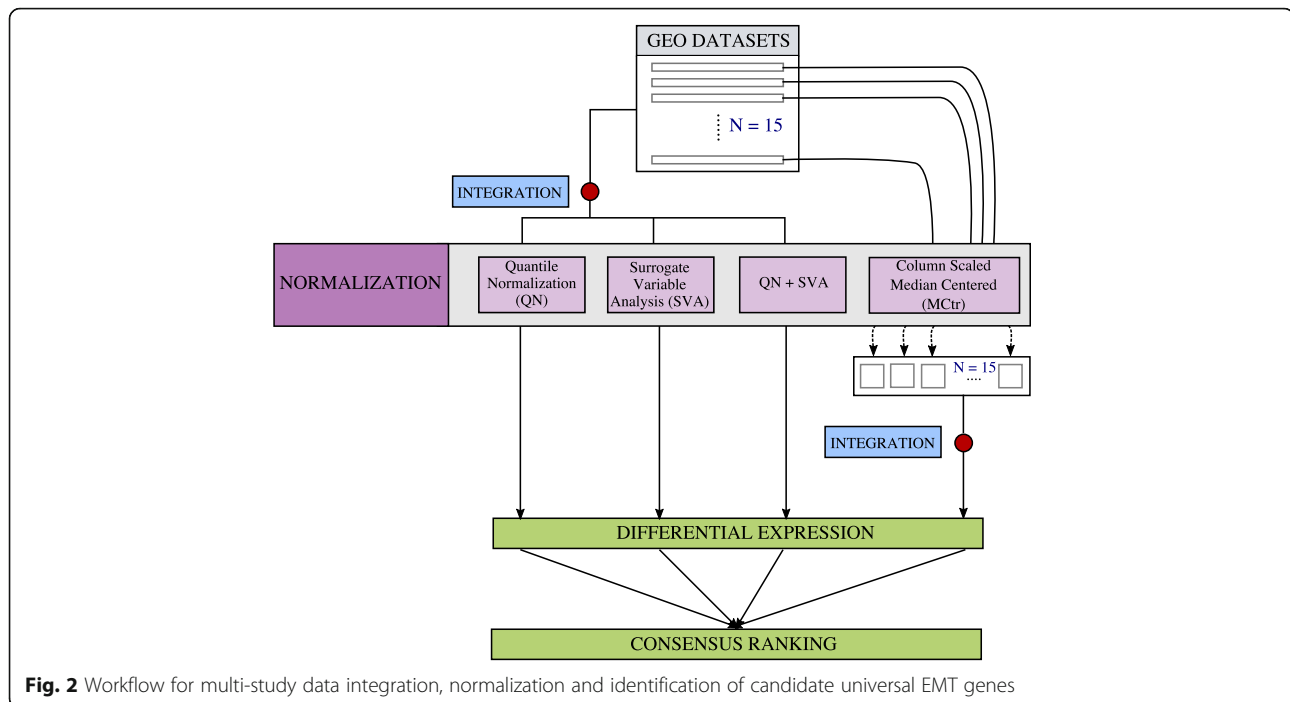


**Fig. 2** Workflow for multi-study data integration, normalization and identification of candidate universal EMT genes

- Sorts each column in  $D$
- Computes mean for each row and assigns it to each element in the row giving  $D'$
- Finally, it rearranges columns in  $D'$  such that it has the same ordering as original  $D$ , thus giving normalized data,  $D_{\text{normalized}}$

At the end of this, each column in  $D$  has the same distribution [33].

#### Surrogate variable analysis

Surrogate variable analysis allows us to preserve the phenotype signal of interest (epithelial and mesenchymal). It estimates known and hidden confounding factors using Singular Value Decomposition on residual variation matrix. We regress out estimated surrogate variables from gene expression data to get SVA normalized gene expression [34].

We also quantile normalize combined data followed by SVA to correct for hidden confounders.

#### Column standardized median centered

Samples from each study are standardized and median centered by gene as described in [35] and combined them.

#### Differential expression analyses and concordance between normalization methods

With each of the normalized dataset, we used a two-sample t-test to identify differentially expressed genes between epithelial and mesenchymal states. Assuming

equal variance, we compared the mean expression of a gene between the two populations. For each gene, we tested:

$$\text{Null Hypothesis : } \mu_{\text{epi}} = \mu_{\text{mes}}$$

$$\text{Alternative : } \mu_{\text{epi}} \neq \mu_{\text{mes}}$$

We ranked genes by raw  $p$ -values. We applied Bonferroni correction for multiple hypothesis testing.

To test concordance between normalization methods, we used spearman rank correlation to test association between gene ranks ( $n = 7276$ ) obtained by different correction methods.

Assuming equal probability of error for each normalization method, we computed average rank for each gene across the four methods that represented the consensus position of each gene according to the differential expression test statistic (Fig. 2).

#### Cluster evaluation of normalized data

To evaluate if normalization improved overall grouping of epithelial and mesenchymal phenotypes together, we clustered each of the normalized data using hierarchical clustering (with all 7276 genes). Next, to evaluate grouping we used Baker Hubert Index for cluster evaluation. Baker Hubert's Index (BH) [36] is an adaptation of Goodman and Kruskal gamma statistic in the context of clustering.

$$BH = \frac{S^+ - S^-}{S^+ + S^-}$$

Here,  $S^+$  is the number of concordant quadruples and  $S^-$  is the number of discordant quadruples. To compute BH, it tests all possible quadruples in the input.

Suppose we were testing quadruple samples  $a, b, c, d$ . And  $d(a, b)$  is the distance between samples  $a$  and  $b$ . A quadruple is concordant if it fulfills one of the following two conditions:

- $d(a, b) > d(c, d)$ ; And  $c$  and  $d$  are in same cluster and  $a$  and  $b$  are in different clusters
- $d(a, b) < d(c, d)$ ; And  $a$  and  $b$  are in same cluster and  $c$  and  $d$  are in different clusters

A quadruple is discordant if:

- $d(a, b) > d(c, d)$ ; And  $a$  and  $b$  are in same cluster and  $c$  and  $d$  are in different clusters
- $d(a, b) < d(c, d)$ ; And  $c$  and  $d$  are in same cluster and  $a$  and  $b$  are in different clusters

Since we were interested in improvement in grouping of epithelial and mesenchymal samples, we used phenotype vector as cluster assignment for evaluation.

#### Gene co-expression module detection using WGCNA

With 200 DE genes from QN + SVA data, unsigned co-expression network was constructed using the WGCNA package in R [37]. Since we used differentially expressed genes, prior to constructing networks, the effect of phenotype (epithelial and mesenchymal) from each gene was removed using a linear model.

$$E_i = \mu + \beta_1 \cdot P_i + \epsilon$$

where,  $\mu$  is the mean effect,  $E_i$  is the expression of a gene in sample  $i$ ,  $\beta_1$  is the regression coefficient of phenotype,  $P_i$  is the phenotype label for sample  $i$  and  $\epsilon \sim N(0, 1)$ . Expression of gene  $\hat{E}$  after regressing out effect of phenotype is given by:

$$\hat{E}_i = E_i - (\mu + \beta_1 \cdot P_i)$$

Next using this, we computed an adjacency matrix  $a_{ij}$  using pearson correlation:

$$a_{ij} = |\text{corr}(e_i, e_j)|^\beta$$

where  $e_n$  is the expression of gene  $n$  and  $\beta$  is the soft-thresholding power for weighted networks. Best scale-free topology fitting index  $R^2$  was obtained at  $\beta = 5.5$  ( $R^2 = 0.77$ ). The adjacency matrix was then transformed to a topological overlap based similarity matrix given by:

$$TOM_{ij} = \sum_u \frac{\sum_k a_{ik} a_{kj} + a_{ij}}{\min\{\sum_k a_{ik}, \sum_k a_{jk}\} + 1 - a_{ij}}$$

The topological overlap between two nodes is the measure of relative interconnectedness. The TOM was then transformed to dissimilarity matrix:

$$\text{diss}TOM_{ij} = 1 - TOM_{ij}$$

Genes were then clustered using average linkage hierarchical clustering.

Co-expression modules were derived from clustering dendrogram using Dynamic Tree Cut with hybrid method. This helped overcome the need for manually selecting a cut-off height. We set minimum module size to 15 since we were looking for modules among 200 genes. The expression profile of each module is represented by its eigengene, which is the first principal component of the module.

#### RT-qPCR

RNA was isolated from cells at ~80% confluency using RNeasy kit (Qiagen) and subsequent cDNA libraries were prepared using Bio-Rad cDNA synthesis kit. TaqMan gene expression assays were used to determine mRNA expression levels using the following probes:  $\beta$ -actin Hs\_1060665\_g1, LSR Hs01076319\_g1, S100A14 Hs04189107, DPYSL3 Hs00181665\_m1, *C1orf116* Hs00539900\_g1, OVOL1 Hs00970334, CDH1 Hs01023894, CDH2 Hs00983056\_m1, ZEB1 Hs00232783\_m1.

*Relative Expression Calculations:* In the qPCR, the target of interest in each sample is measured using at least three biological replicates. The Ct value for each biological replicate is calculated as an average of three technical replicates. Then the Ct value of each biological replicate is normalized to  $\beta$ -actin by subtracting it from the corresponding Ct value of  $\beta$ -actin ( $-\Delta Ct$ ). The two groups of interest are compared using a Student's t-test. The values plotted in the graph are the average of the base 2 anti-log transformations of  $-\Delta Ct$  for the biological replicates of interest divided by the average of the base 2 anti-log of  $-\Delta Ct$  for the reference group. The standard errors of the mean are determined from biological replicates.

#### Western blot

Protein extracts were prepared using Frackleton-lysis buffer with protease inhibitors (Thermo Scientific 78,410), and samples were electrophoresed on 4–15% SDS-PAGE (Bio-Rad), transferred to a nitrocellulose membrane and blocked with casein blocking buffer (Sigma B6429). The list of antibodies used for western blotting is in Additional file 2: Table S6. The Licor



Odyssey fluorescence scanner was used for visualizing the westerns.

#### siRNA knockdown of *C1orf116*

*C1orf116* siRNA (ThermoFisher, cat#: 4,392,420) with RNAiMAX transfection reagent (ThermoFisher) was used for siRNA transfections. Some alterations were made to manufacturer's recommended protocol. Cells were seeded at a density result in 50% confluency the following day. Using a 6 well plate, 9 ul of RNAiMAX reagent and 3 ul (30 pmol) of siRNA (each diluted in 150 ul of Opti-MEM media) was added to each well the day after seeding. 72 h later RNA was isolated (Qiagen, Rneasy mini kit) from plates and gene expression was analyzed.

#### *C1orf116* expression in cancer patient data

We identified publicly available published cancer patient (breast, prostate, esophageal, liver, colorectal, and lung) gene expression studies with at least 150 patients on OncoPrint [38]. Gene expression data for studies (GSE17536 [39], GSE11121 [40], GSE25066 [41], GSE22358 [42], GSE7390 [43], GSE68465 [44], GSE31210 [45], and GSE21034 [46]) available on GEO were obtained using the GEOquery R package [47]. Probeset IDs corresponding to *C1orf116* were used. Gene level expression was obtained by aggregating multiple probe expression values with median. Wilcoxon rank sum test was used to test association between expression of *C1orf116* and grade, smoking status and cancer sample site. We also looked at association between tumor grade and *C1orf116* expression in 4 breast cancer, 1 colorectal cancer and 1 lung cancer studies from OncoPrint. We adjust Wilcoxon rank sum *p*-values with bonferroni correction for a total of 23 tests performed for clinical associations (Table 2, Additional file 3: Table S7 and Additional file 4: Figure S7).

#### Results

We identified publicly available gene expression microarray datasets that queried gene expression of cell lines induced to undergo EMT [7–21]. We confirmed the phenotype of the samples by referring to associated publications for immunohistochemistry staining and/or protein expression of known epithelial or mesenchymal markers (Table 1, Additional file 2: Table S1). 95 cell line observations (45 unique samples and 50 replicates) from 15 datasets that showed sufficient evidence of correct phenotypic labeling included 49 cell lines of epithelial phenotype and 46 cell lines of mesenchymal phenotype.

#### Normalization methods show consistency in signal

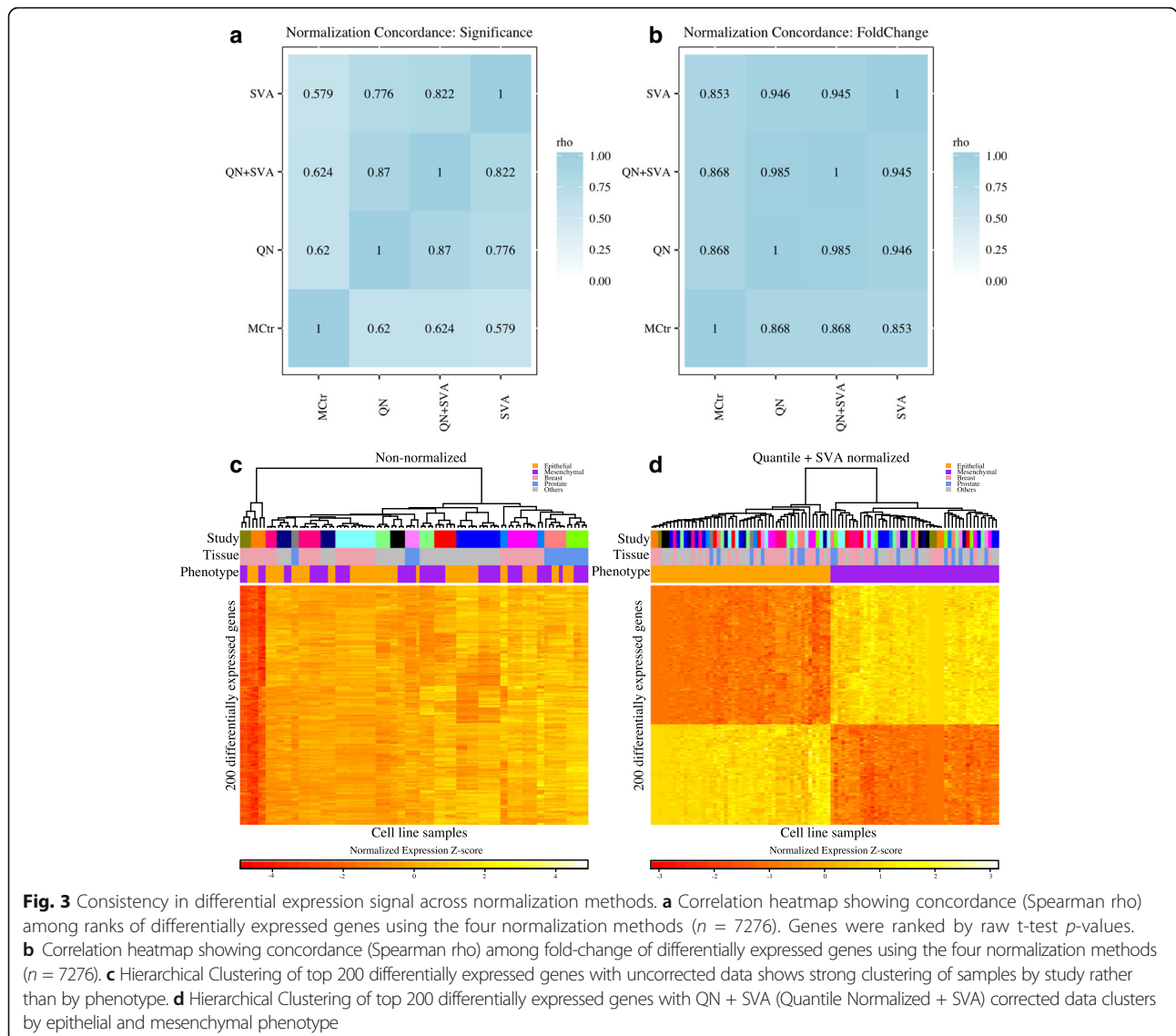
Technical variability in the form of noise and batch-effects is inherent in gene expression data. We performed

**Table 2** Association of *C1orf116* expression in lung and prostate cancer patients

Test group	Wilcoxon rank sum <i>p</i> -value	Bonferroni adjusted <i>p</i> -value
Lung cancer (Director's Lung Challenge): grade [44]		
Grade 1 vs Grade 2	1.4191e-06	3.27E-05
Grade 2 vs Grade 3	1.1481e-10	2.65E-09
Grade 1 vs Grade 3	2.6121e-17	6.00E-16
Lung cancer (Director's Lung Challenge): Smoking Status [44]		
Never vs Past	0.006	1.38E-01
Past vs Current	0.006	1.38E-01
Never vs Current	0.0002	4.60E-03
Lung cancer (Okayama): Smoking status [45]		
Never smoker vs ever smoker	0.0586	1E + 00
Prostate cancer (Taylor): Tumor type [46]		
Primary vs Metastatic	0.0340	7.82E-01

rigorous confounding factor correction to make gene expression comparisons between epithelial and mesenchymal samples that came from different studies, platforms, and cell lines. We used simple normalization methods including column standardized mean centered (MCTR) [35] and Quantile Normalization (QN) [33] and more rigorous methods that included Surrogate Variable Analysis (SVA) [34] and combination of QN followed by SVA (QN + SVA). With each normalization method (MCTR, QN, SVA, QN + SVA), we compared mean expression of epithelial and mesenchymal cell lines by a two-sample *t*-test for differential expression. We evaluated concordance among normalization methods to determine signal robustness – any individual method may be subject to false positives due to different patterns such as outliers, batch effects, etc. For this, we restricted our analysis to 7276 genes that were common across all studies. We used Spearman correlation to test association between raw test statistics ( $n = 7276$  genes) obtained from two-sample *t*-test from each of type of normalized data. Test-statistic distributions from individual normalization methods were significantly correlated with each other ( $p$ -value  $< 2.2e-16$ ,  $n = 7276$ ). This indicates that signal produced by data normalized using a particular method is consistent with others (Fig. 3, Additional file 5: Figure S1, Additional file 6: Figure S2 and Additional file 7: Figure S3).

Next, to assess if normalization improved overall grouping of epithelial and mesenchymal phenotypes together, we clustered samples from each of the normalized datasets using hierarchical clustering (using all 7276 genes). Next, to evaluate this grouping we used the Baker Hubert Index (BH) with known phenotype vector as group assignments. Values of the BH index range



from  $-1$  to  $1$ , with larger values indicating better grouping [48]. Table 3 shows that grouping of samples by phenotype (epithelial or mesenchymal) is considerably improved in normalized datasets in comparison to non-normalized data. QN + SVA performs the best, followed by SVA, MCtr and QN.

**Differential expression analyses reveal universal EMT genes across multiple carcinoma types**

With every form of normalized data (MCtr, QN, SVA, QN + SVA), we determined differentially expressed genes between epithelial and mesenchymal cell phenotype by a

two-sample t-test. A gene list ranked by raw  $p$ -values from the t-test was generated for each normalization method. Assuming equal likelihood of error in correction methods (Fig. 2), for each gene we assigned a differential rank that was the average of  $p$ -value ranks from all four normalization methods. This was used to generate a final integrated ranked gene list (Additional file 8: Table S2).

We defined a candidate universal EMT gene list by the top 200 genes from the integrated gene list (absolute fold change  $>1.2$  and FDR  $< 0.005$  in SVA, QN + SVA and MCtr normalized data) (Additional file 8: Table S2). These genes are representative of global differential

**Table 3** Evaluation of sample grouping (with 7276 genes) using Baker Hubert index and phenotype information

	No normalization	Quantile Normalization (QN)	Surrogate Variable Analysis (SVA)	QN + SVA	Median Centered Column Scaled
Baker Hubert Index	0.0001	0.047	0.864	0.7995	0.0705

EMT patterns independent of cell line origin and treatment modality.

Cancer cells recruit developmental pathways and processes to acquire migratory and invasive properties. To determine if the candidate gene list contained groups of genes working together and shared common biological functions we tested enrichment it's enrichment for Hallmark genesets (MSigDB) defined and curated by the Broad Institute [49] using a right-tailed Fisher's exact test. The most significantly enriched gene set was epithelial to mesenchymal transition (Odds ratio = 18.3575636, FDR = 4.92E-31). Among the other hallmark gene sets, we found increased representation (FDR < 10%) of several EMT related pathways including estrogen responsive genes (early and late), genes upregulated in response to low oxygen levels (hypoxia) and others [5, 50–57] (Table 4). We also found that specific estrogen responsive genes (early and late) were differentially expressed even when restricted just to the prostate cancer samples (Additional file 9: Figure S6) indicating this enrichment was not due exclusively to breast cancer cell lines in our combined analysis. When tested for GO biological processes, we found enrichment (FDR < 10%) for several developmental terms including epidermis development, anatomical structure morphogenesis and organ development

(Additional file 10: Table S3). This further confirms that our analyses capture comprehensive signals in identifying changes in gene expression patterns across cancer types during EMT.

Among genes on our candidate gene list, we found known epithelial- and mesenchymal-specific genes such as E-cadherin (*CDH1*), Zinc Finger E-Box Binding Homeobox 1 (*ZEB1*), Vimentin (*VIM*), Transforming Growth Factor, Beta 1 (*TGFB1*), Tissue Inhibitor Of Metalloproteinase 1 (*TIMP1*) [5, 58], N-cadherin (*CDH2*) (Table 5). We also observed enrichment of collagen genes that are known to be associated with cell adhesion and migration amongst DE genes (Fisher's exact *p*-value 1.124e-05) [5]. In addition, we also found known EMT related transcription factors such as *ZEB1*, *ETS1* and *LSR* in our candidate gene list.

We also compared our list of genes to the core EMT gene signature described by Groger et al. [27]. We found 43 common genes from their study (Additional file 11: Table S4). These included genes such as *CDH1*, *CDH2*, *VIM*, *LSR* and some collagen genes. Several known EMT genes such as *TGFB*, *TIMP1*, *ETS1* that were found in universal EMT genes were missing from their list. Some other genes such as *S100A14*, *DPYSL3* and *C1orf116* (Additional file 12: Figure S4 and Additional file 13: Figure S5) that we validate as differential EMT genes in our study, were also not found in their core gene list.

**Table 4** Enriched MsigDB Hallmark genesets

Geneset	<i>p</i> -values	oddsratio	FDR	Genes in set
HALLMARK Epithelial mesenchymal transition	9.84E-33	18.3575636	4.92E-31	<i>CD59</i> , <i>CDH11</i> , <i>CDH2</i> , <i>COL1A1</i> , <i>COL1A2</i> , <i>COL4A2</i> , <i>COL5A1</i> , <i>COL6A3</i> , <i>CTGF</i> , <i>CYR61</i> , <i>DAB2</i> , <i>DPYSL3</i> , <i>EDIL3</i> , <i>EMP3</i> , <i>ENO2</i> , <i>FAP</i> , <i>FBN1</i> , <i>FBN2</i> , <i>FERMT2</i> , <i>GEM</i> , <i>GJA1</i> , <i>GREM1</i> , <i>LGALS1</i> , <i>LOX</i> , <i>MMP14</i> , <i>MMP2</i> , <i>PCOLCE</i> , <i>PCOLCE2</i> , <i>PLAUR</i> , <i>PLOD1</i> , <i>PMP22</i> , <i>POSTN</i> , <i>SERPINE1</i> , <i>SERPINE2</i> , <i>SLIT2</i> , <i>SPARC</i> , <i>SPOCK1</i> , <i>TGFB1</i> , <i>TIMP1</i> , <i>VCAN</i> , <i>VIM</i> , <i>WNT5A</i>
HALLMARK Estrogen response late	9.36E-06	4.332224532	0.00019652	<i>ALDH3A2</i> , <i>ASS1</i> , <i>CDH1</i> , <i>CELSR2</i> , <i>LLGL2</i> , <i>LSR</i> , <i>MAPK13</i> , <i>PLXNB1</i> , <i>RAPGEFL1</i> , <i>SCNN1A</i> , <i>SLC22A5</i> , <i>SLC27A2</i> , <i>ST14</i> , <i>TOB1</i> , <i>TRIM29</i>
HALLMARK Apical junction	1.18E-05	4.516129032	0.00019652	<i>AKT3</i> , <i>CDH1</i> , <i>CDH11</i> , <i>CLDN7</i> , <i>FBN1</i> , <i>GRB7</i> , <i>JAM3</i> , <i>JUP</i> , <i>MAPK13</i> , <i>MMP2</i> , <i>MPZL2</i> , <i>PVRL3</i> , <i>SLIT2</i> , <i>VCAN</i>
HALLMARK UV response dn	8.16E-05	4.23768997	0.001019448	<i>AKT3</i> , <i>COL1A1</i> , <i>COL1A2</i> , <i>CYR61</i> , <i>DAB2</i> , <i>FZD2</i> , <i>GJA1</i> , <i>HAS2</i> , <i>KCNMA1</i> , <i>MAP1B</i> , <i>PMP22</i> , <i>SERPINE1</i>
HALLMARK Estrogen response early	0.000247578	3.495078664	0.002475779	<i>AQP3</i> , <i>CELSR2</i> , <i>CLDN7</i> , <i>ELF3</i> , <i>GJA1</i> , <i>KRT15</i> , <i>PMAIP1</i> , <i>RAPGEFL1</i> , <i>SCNN1A</i> , <i>SLC22A5</i> , <i>SLC27A2</i> , <i>TOB1</i> , <i>WWC1</i>
HALLMARK Hypoxia	0.000436298	3.276838008	0.003635818	<i>AKAP12</i> , <i>CHST2</i> , <i>COL5A1</i> , <i>CTGF</i> , <i>CYR61</i> , <i>ENO2</i> , <i>ETS1</i> , <i>HMOX1</i> , <i>KDELRL3</i> , <i>LOX</i> , <i>PLAUR</i> , <i>SERPINE1</i> , <i>SRPX</i>
HALLMARK Inflammatory response	0.000679488	3.786760716	0.004246802	<i>CD70</i> , <i>CHST2</i> , <i>EMP3</i> , <i>FZD5</i> , <i>HAS2</i> , <i>HRH1</i> , <i>MMP14</i> , <i>PLAUR</i> , <i>SERPINE1</i> , <i>TIMP1</i>
HALLMARK KRAS signaling up	0.00061698	3.554348835	0.004246802	<i>AKAP12</i> , <i>EPB41L3</i> , <i>ETS1</i> , <i>GFPT2</i> , <i>GNG11</i> , <i>JUP</i> , <i>MAP7</i> , <i>MPZL2</i> , <i>PLAUR</i> , <i>TMEM158</i> , <i>TRIB2</i>
HALLMARK Angiogenesis	0.003822541	7.2	0.02123634	<i>JAG2</i> , <i>POSTN</i> , <i>TIMP1</i> , <i>VCAN</i>
HALLMARK Complement	0.00451196	3.068992514	0.022559801	<i>CD59</i> , <i>COL4A2</i> , <i>CTSD</i> , <i>MMP14</i> , <i>PLAUR</i> , <i>SERPINE1</i> , <i>TIMP1</i> , <i>TIMP2</i> , <i>ZEB1</i>
HALLMARK Myogenesis	0.00594623	2.929880329	0.027028319	<i>COL1A1</i> , <i>COL4A2</i> , <i>COL6A3</i> , <i>ERBB3</i> , <i>MEF2C</i> , <i>NCAM1</i> , <i>PDLIM7</i> , <i>SPARC</i> , <i>TGFB1</i>
HALLMARK TGF beta signaling	0.010673511	4.097902098	0.044472964	<i>BCAR3</i> , <i>CDH1</i> , <i>SERPINE1</i> , <i>SMURF2</i> , <i>TGFB1</i>



**Table 5** Rank of known epithelial and mesenchymal specific genes and DE genes found in Hallmark Epithelial to mesenchymal transition [73]

Gene Symbol	Order in average rank	Gene Symbol	Order in average rank	Gene Symbol	Order in average rank
<i>EMP3</i>	3	<i>PCOLCE2</i>	45	<i>VIM*</i>	144
<i>VCAN</i>	4	<i>FAP</i>	54	<i>FERMT2</i>	147
<i>GEM</i>	6	<i>CDH11</i>	73	<i>POSTN</i>	150
<i>CDH2*</i>	11	<i>TGFB1*</i>	81	<i>FBN2</i>	155
<i>ZEB1*</i>	12	<i>SPARC</i>	84	<i>GJA1</i>	159
<i>SPOCK1</i>	13	<i>CYR61</i>	90	<i>SERPINE1</i>	161
<i>COL4A2</i>	14	<i>WNT5A</i>	95	<i>DAB2</i>	168
<i>FBN1</i>	15	<i>CD59</i>	98	<i>COL1A1</i>	171
<i>PMP22</i>	21	<i>GREM1</i>	106	<i>MMP2</i>	174
<i>COL5A1</i>	22	<i>PLAUR</i>	108	<i>PCOLCE</i>	181
<i>CDH1*</i>	24	<i>CTGF</i>	118	<i>ENO2</i>	187
<i>SLIT2</i>	33	<i>COL1A2</i>	120	<i>LGALS1</i>	191
<i>EDIL3</i>	36	<i>PLOD1</i>	124	<i>SERPINE2</i>	162
<i>DPYSL3</i>	42	<i>MMP14</i>	127		
<i>COL6A3</i>	43	<i>LOX</i>	129		

\*commonly used EMT marker genes

#### Candidate gene list identified genes previously unknown in prostate cancer EMT

In addition to genes well established in the process of EMT, we also identified genes that had only been described in EMT in a subset of cancer types, including two epithelial specific genes, lipolysis stimulated lipoprotein receptor (*LSR*) and S100 calcium binding protein A14 (*S100A14*), and one mesenchymal specific gene, dihydropyrimidinase-like 3 (*DPYSL3*). Previous studies have investigated role of *LSR* in breast cancer EMT [59], and *S100A14* has been examined in pancreatic and cervical cancer [60, 61]. Previous studies have indicated involvement of *DPYSL3* in malignant pancreatic and gastric tumors [62, 63].

We validated the expression of these genes in an in vitro model of prostate cancer EMT. mRNA and protein expression levels of these genes were determined in one epithelial and two mesenchymal prostate cancer cell line PC3 derivatives. PC3-Epi is an expansion of a highly epithelial clone from the parental PC3 population. The mesenchymal derivatives were generated from PC3 cells by M2 macrophage co-cultures (PC3-EMT) and Taxol treatment and subsequent resistance (PC3-TxR) [20, 64]. RT-qPCR of canonical epithelial and mesenchymal genes, *OVOL1*, *OVOL2*, *CDH1*, *ZEB1*, and *CDH2*, confirmed the appropriate phenotypic states for these cell lines (Fig. 4a). Elevated levels of *S100A14* mRNA was observed in PC3-Epi compared to mesenchymal PC3-

EMT and PC3-TxR. Similarly, mRNA expression of epithelial gene *LSR* was found to be higher in PC3-Epi than in its mesenchymal counterparts, PC3-EMT and PC3-TxR (Fig. 4b).

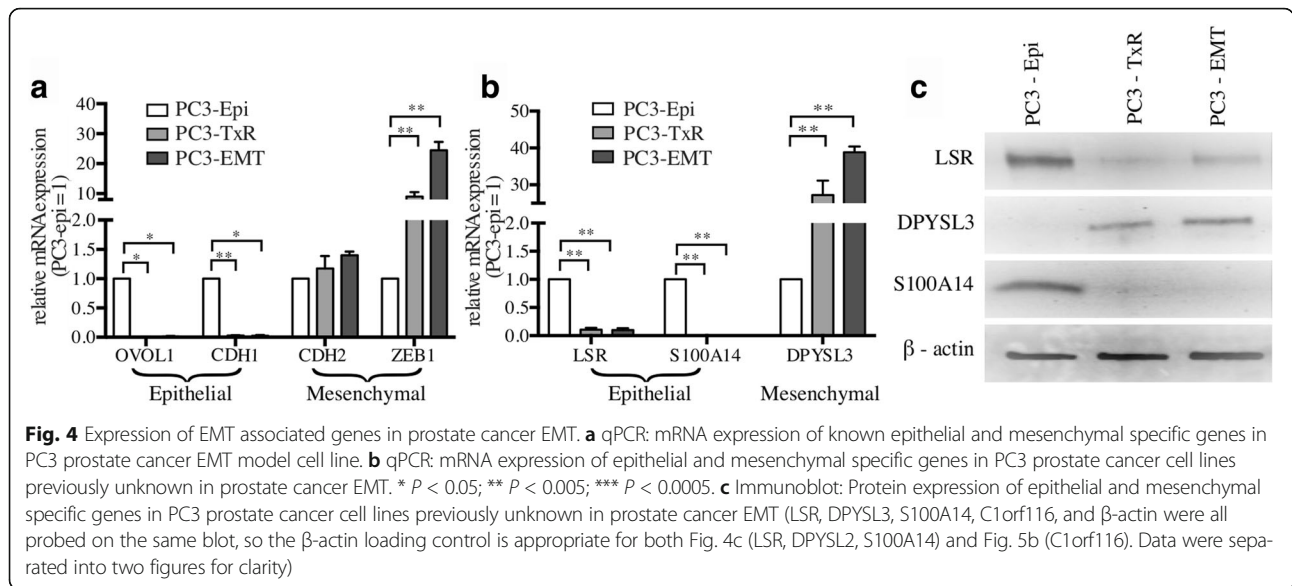
Conversely, the mesenchymal gene *DPYSL3* was extremely upregulated in PC3-EMT and PC3-TxR than in PC3-Epi (Fig. 4b). These results were supported by western blot analysis, which demonstrated protein levels mirrored the mRNA expression (Fig. 4c).

#### *C1orf116* was discovered to be a novel EMT regulator

Our candidate gene list also contained genes that have not been previously described as related to the EMT process in any cancer type or in any physiologic process. One of these novel candidate EMT genes, *C1orf116* (also known as *SARG*), is a poorly characterized gene with only one PubMed listed publication [65]. We first validated our finding from microarray data using the PC3 in vitro model of EMT and found increased mRNA expression in PC3-Epi cells compared to PC3-emt (1.3 fold) and PC3-TxR (8.8 fold). These results were supported by elevated protein expression of *C1orf116* in PC3-epi cells (Fig. 5a-b).

Increased expression *C1orf116* in epithelial cells confirmed of it as an epithelial marker gene. We applied gene network analysis [37], that revealed weighted co-expression gene modules (groups of co-expressed genes) and showed that *C1orf116* clustered with other epithelial genes including *CDH1*, *LSR*, *S100A14* and others (Additional file 14: Table S5, Fig. 6). *LSR* and *S100A14* were among the known-unknown genes whose expression was validated in PC3 cell lines. This confirmed its association with other epithelial genes universal across other disease types. Through manual literature search, we identified that a subset of the *C1orf116* module gene list have been shown to be associated with multiple cancer types. Among other genes in the modules, *SH2D3A*, *APIM2*, *CDS1* and *SCNN1A* haven't been previously studied in cancer biology. This shows that in addition to being a novel EMT regulator in prostate cancer, *C1orf116* could have broad effects across multiple cancer types.

Next, we interrogated the possible role of *C1orf116* in in vivo malignant progression. For this, we identified gene expression studies with at least 150 patients that also had information on tumor grade and expression data for *C1orf116* and were able to find breast, prostate, colorectal and lung cohorts (Additional file 4: Figure S7). We found that *C1orf116* expression is decreased in metastatic lesions compared to localized tumors in prostate cancer patients (Fig. 7a) [46]. Likewise, *C1orf116* expression decreased with increasing cancer grade in patients with lung cancer (Fig. 7b) [44]. Studies have shown that lung cancer patients with history of smoking



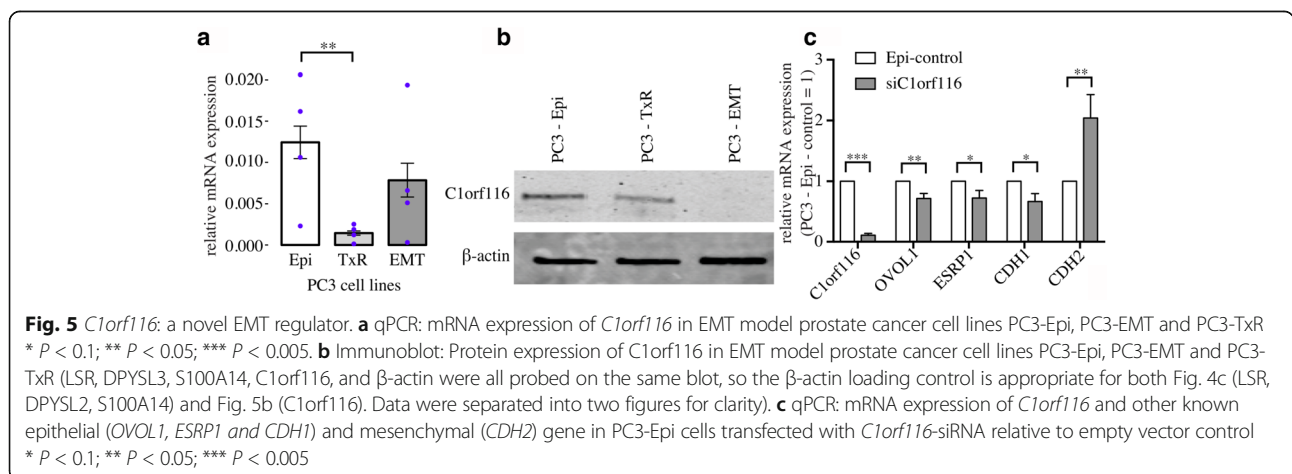
tobacco/cigarette exhibit lower expression levels of E-cadherin and higher levels of mesenchymal markers such as vimentin [66, 67]. Previous studies have also indicated that cigarette smoking can induce EMT in non-small cell lung cancer [68]. Analogous to these findings, we observed reduced expression of *C1orf116* among lung cancer patients with smoking habits (Fig. 7c-d) [44, 45]. In some breast cancer datasets expression of *C1orf116* increased with increasing cancer grade (Additional file 3: Table S7 and Additional file 4: Figure S7). This suggested that in addition to expression changes in in vitro cell line models, changes in *C1orf116* expression could potentially have a functional role in clinically-important disease progression in cancer patients.

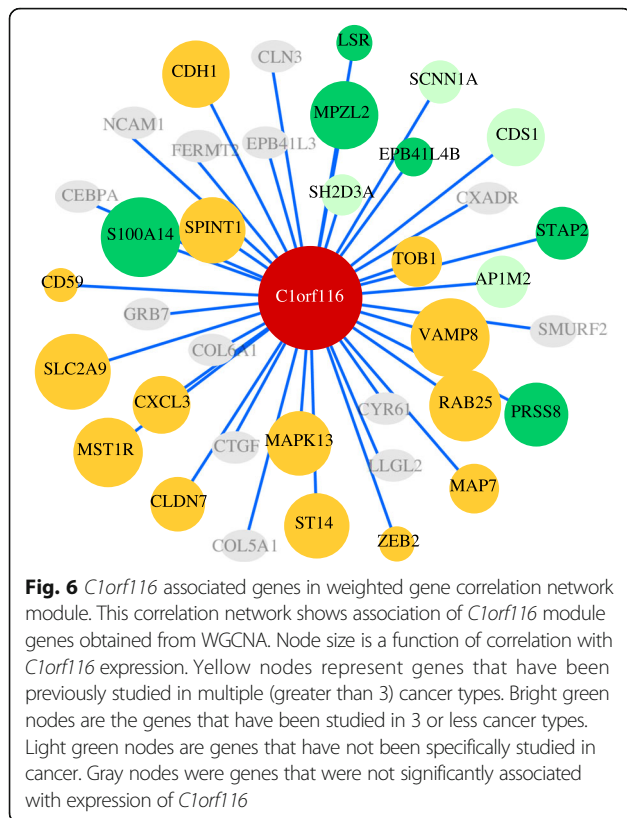
To test the role of *C1orf116* as a driver of an epithelial phenotype, we used siRNA-mediated knockdown of the gene in PC3-Epi cells. We found that siRNA-mediated

knockdown of *C1orf116* expression resulted in decreased expression of epithelial markers *OVOL1*, *ESRP1*, and *CDH1*, and increased expression of mesenchymal marker *CDH2* (Fig. 5c). This suggests that *C1orf116* plays a functional role in maintaining epithelial phenotype. Significant upregulation of mesenchymal genes in response to *C1orf116* knockdown indicates it as a novel regulator of EMT.

### Discussion

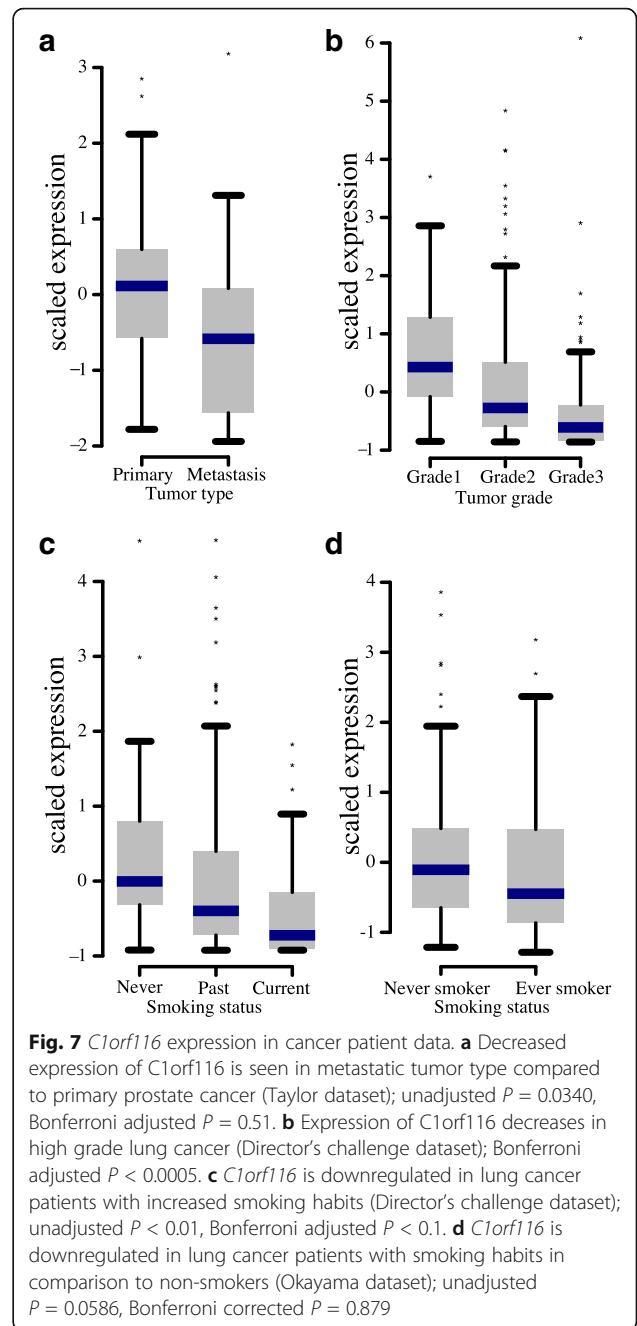
EMT may be an early step in cancer metastasis and has been associated with chemoresistance and disease progression [69, 70]. Though EMT is common among all solid tumor types and is essential in early development, common drivers of EMT across multiple cancer types have not been described. Several studies have investigated EMT in cell lines from within a single disease type. Although most studies have been confined to very





small sample size. To address this, we systematically integrate multiple EMT studies to increase power and identify novel drivers of EMT universal to all cancer types.

A significant challenge in multi-study analysis comes from various sources of heterogeneity arising from study specific technical and biological variation. Biological variation interferes with analyses, especially when it is not the signal of interest. We employed two strategies to address various sources of heterogeneity and noise. First, we chose stringent normalization methods that have been shown to reduce the influence of such heterogeneity (SVA, quantile normalization, and scaled median centering). We recognize that these methods may have their failure modes and limitations. Therefore, we defined our final differentially expressed gene list from consensus ranking across all four normalization schemes. Thus even if a single method introduced an error or failed to account for a particular effect, the final gene list may be more robust than results from any individual method. However, technical variation and experimental heterogeneity may still influence the results of our analysis, as no method has been shown to fully remove such effects from expression data. Therefore, experimental validation and comparison with external functional annotation were important.



Integrating across multiple studies did improve power and helped us detect novel genes that showed consistent effect across multiple studies, which could be concealed in a single study. We found three groups of genes in the EMT differentially expressed list: a) known EMT genes (e.g. *CDH1*, *ZEB1*, *TGFB*, *CDH2*, *VIM*, *TIMP1*), b) EMT genes previously unknown in prostate cancer (*LSR*, *S100A14*, *DPYSL3*) and c) novel EMT genes (including *C1orf116*).

We confirmed our discovery of unknown EMT genes in prostate cancer by testing expression of *LSR*, *S100A14*, and *DPYSL3* in a PC3 prostate cancer cell line

model of EMT. Previous studies have shown that LSR suppresses EMT phenotype in claudin-low breast cancer cell lines [59]. *S100A14* has been studied in breast cancer progression and is shown to be involved in EMT in human cervical and pancreatic cancer cells [60, 61, 71]. *DPYSL3* is associated with malignant gastric and pancreatic tumors [62, 63]. Moreover studies suggest that mRNA expression of *DPYSL3* is positively correlated with Vascular Endothelial Growth Factor (*VEGF*), a gene thought to be involved in EMT [72]. This data indicates that our method bridged EMT cancer biology across different disease types and captures global expression patterns in EMT (Additional file 12: Figure S4A-C).

We confirmed discovery of *C1orf116* as epithelial specific gene by testing its expression in PC3 in vitro model of EMT. siRNA knockdown of *C1orf116* in PC3 epithelial cell lines showed loss of epithelial markers and gain of mesenchymal markers thereby confirming its functional role as a negative driver of EMT. Clinical data from breast, prostate cancer and lung cancer patients also suggested that changes in expression of *C1orf116* could have functional implications in disease progression.

Altogether, through this study we have found genes whose effects are represented by multiple cancer types (breast, prostate, liver, colon, esophagus and retinal pigment). We have also validated expression of some genes in an in vitro prostate cancer cell line model and potential relevance in vivo data from three tissues, including one (lung) that was not represented among our cell line data. However, these effects might not necessarily be extrapolated for cancer types not included in this study. As data become available for other tissues and cancers, further analysis can be performed.

## Conclusions

Using multi-study integration approach, we identified consensus ranked universal EMT genes. This gene list comprised of a) known EMT genes that included *CDH1*, *ZEB1* and *CDH2* b) genes studied in a subset of carcinomas, unknown in prostate cancer: *LSR*, *S100A14* and *DPYSL3* and c) novel unknown EMT and cancer genes such as *C1orf116*. siRNA experiments indicate it to be a potential novel regulator of EMT. Patient gene expression data shows that reduced expression of *C1orf116* is associated with poor prognosis in lung and prostate cancer (unadjusted Wilcoxon rank sum  $p$ -value <0.05). In conclusion, our approach of statistical analysis and functional validation identified universal EMT genes and candidate global regulatory genes, thereby both extending current knowledge of EMT and showed preliminary evidence of disease progression in cancer.

## Additional files

**Additional file 1: Table S1.** Dataset information – Extended table. (XLSX 33 kb)

**Additional file 2: Table S6.** List of antibodies used in immunoblot. (XLSX 36 kb)

**Additional file 3: Table S7.** Association of *C1orf116* expression in lung and prostate cancer patients. (XLSX 9 kb)

**Additional file 4: Figure S7.** *C1orf116* expression in clinical patient data from breast and colorectal cancer. (PDF 25 kb)

**Additional file 5: Figure S1.** Hierarchical Clustering of top 200 differentially expressed genes with data corrected by quantile normalization. (PDF 429 kb)

**Additional file 6: Figure S2.** Hierarchical Clustering of top 200 differentially expressed genes with data corrected by SVA (Surrogate Variable Analysis) normalization. (PDF 122 kb)

**Additional file 7: Figure S3.** Hierarchical Clustering of top 200 differentially expressed genes with data corrected by MCtr (Median Centered Column Scaled) normalization. (PDF 122 kb)

**Additional file 8: Table S2.** Gene ranks – fold change and significance based. (XLSX 1503 kb)

**Additional file 9: Figure S6.** Expression of Estrogen responsive genes - (A) early and (B) late in prostate cancer cell line samples from integrated data. (PDF 115 kb)

**Additional file 10: Table S3.** Gene set enrichment with GO Biological Processes term. (XLSX 36 kb)

**Additional file 11: Table S4.** Common genes with Groger et al. study and 200 DE genes. (XLSX 32 kb)

**Additional file 12: Figure S4.** Expression of EMT genes previously unknown in prostate cancer in integrated cell lines data. Expression of *LSR* (A), *S100A14* (B) and *DPYSL3* (C) in breast, prostate and others (retinal pigment, liver, colon and esophageal) cancer cell lines from QN + SVA normalized integrated data. (PDF 97 kb)

**Additional file 13: Figure S5.** Expression of *C1orf116* in breast, prostate and others (retinal pigment, liver, colon and esophageal) cancer cell lines from integrated data. (PDF 45 kb)

**Additional file 14: Table S5.** *C1orf116* module genes obtained from Weighted Gene Co-expression analysis. (XLSX 42 kb)

## Abbreviations

EMT: Epithelial to mesenchymal transition; MCtr: Median Centered Column Scaled; MET: Mesenchymal to epithelial transition; QN: Quantile Normalization; RT-qPCR: Reverse transcription quantitative polymerase chain reaction; SVA: Surrogate Variable Analysis; WGCNA: Weighted Gene Coexpression Network Analysis

## Acknowledgements

We would like to thank members of Battle and Pienta lab for their inputs.

## Funding

K.J. Pienta is supported by the National Cancer Institute (CA093900, CA163124, U54CA143803, CA143055) and the Prostate Cancer Foundation. Alexis Battle is supported by R01 MH101814 (NIH/NIMH), R01 HG008150 (NIH/NIGMS), 1R01GM118568-01 (NIH/NIGMS) and R01 MH101820 (NIH). Sarah R. Amend is supported by an American Cancer Society Postdoctoral Fellowship (PF-16025-01-CSM). There was no role of the funding body in the design of the study and collection, analysis, and interpretation of data and in writing the manuscript.

## Availability of data and materials

All data generated or analysed during this study are included in this published article [and its supplementary information files].

## Authors' contributions

PP, AB and KJP conceived and designed the study. PP performed computational analysis including normalization, differential expression, concordance and WGCNA. RT-qPCR, immunoblot and siRNA experiments were performed by JH. PP, JH and SRA analyzed clinical patient data. PP



wrote the manuscript. JH helped with writing the initial draft of manuscript. SRA helped with drafting of manuscript and critical reviews. AB and KJP helped with critical review of manuscript. All authors read and approved the final manuscript.

#### Competing interests

AB holds stock in Google Inc.

#### Consent for publication

Not applicable.

#### Ethics approval and consent to participate

Not applicable.

#### Publisher's Note

Springer Nature remains neutral with regard to jurisdictional claims in published maps and institutional affiliations.

#### Author details

<sup>1</sup>Department of Computer Science, Johns Hopkins University, Baltimore, MD 21218, USA. <sup>2</sup>Department of Urology, Johns Hopkins University School of Medicine, Baltimore, MD 21287, USA.

Received: 24 August 2016 Accepted: 8 June 2017

Published online: 26 June 2017

#### References

- Mehlen P, Puisieux A. Metastasis: a question of life or death. *Nat Rev Cancer*. 2006;6:449–58.
- Tsai JH, Yang J. Epithelial-mesenchymal plasticity in carcinoma metastasis. *Genes Dev*. 2013;27:2192–206.
- Chaffer CL, Weinberg R a. A Perspective on Cancer Cell Metastasis. *Science* (80- ). 2011;331:1559–64.
- Thiery JP, Acloque H, Huang RYJ, Nieto MA. Epithelial-Mesenchymal transitions in development and disease. *Cell*. 2009;139:871–90.
- Kalluri R, Weinberg RA. The basics of epithelial-mesenchymal transition. *J Clin Invest*. 2009;119:1420–8.
- Craene B De, Bex G. Regulatory networks defining EMT during cancer initiation and progression. *Nat Rev Cancer Nature Publishing Group*. 2013; 13:97–110.
- Bergamaschi A, Kim YH, Kwei KA, La Choi Y, Bocanegra M, Langerød A, et al. CAMK1D amplification implicated in epithelial-mesenchymal transition in basal-like breast cancer. *Mol Oncol*. 2008;2:327–39.
- Choi Y La, Bocanegra M, Kwon MJ, Shin YK, Nam SJ, Yang JH, et al. LYN is a mediator of epithelial-mesenchymal transition and a target of dasatinib in breast cancer. *Cancer Res* 2010;70:2296–2306.
- Papageorgis P, Lambert AW, Ozturk S, Gao F, Pan H, Manne U, et al. Smad signaling is required to maintain epigenetic silencing during breast cancer progression. *Cancer Res*. 2010;70:968–78.
- Deshiere A, Duchemin-Pelletier E, Spreux E, Ciaïs D, Combes F, Vandenbrouck Y, et al. Unbalanced expression of CK2 kinase subunits is sufficient to drive epithelial-to-mesenchymal transition by Snail1 induction. *Oncogene*. 2013;32: 1373–83.
- Cai J, Guan H, Fang L, Yang Y, Zhu X, Yuan J, et al. MicroRNA-374a activates Wnt/β-catenin signaling to promote breast cancer metastasis. *J Clin Invest*. 2013;123:566–79.
- Andarawewa KL, Erickson AC, Chou WS, Costes SV, Gascard P, Mott JD, et al. Ionizing radiation predisposes nonmalignant human mammary epithelial cells to undergo transforming growth factor ??-induced epithelial to mesenchymal transition. *Cancer Res*. 2007;67:8662–70.
- Joyce T, Cantarella D, Isella C, Medico E, Pintzas A. A molecular signature for epithelial to Mesenchymal transition in a human colon cancer cell system is revealed by large-scale microarray analysis. *Clin Exp Metastasis*. 2009;26:569–87.
- Hwang W, Yang M, Tsai M, Lan H, Su S, Chang S, et al. SNAIL regulates interleukin-8 expression, stem celllike activity, and tumorigenicity of human colorectal carcinoma cells. *Gastroenterology* 2011;141:279–291, 291–5.
- Ohashi S, Natsuzaka M, Naganuma S, Kagawa S, Kimura S, Itoh H, et al. A NOTCH3-mediated squamous cell differentiation program limits expansion of EMT-competent cells that express the ZEB transcription factors. *Cancer Res*. 2011;71:6836–47.
- van Zijl F, Mall S, Machat G, Pirker C, Zeillinger R, Weinhaeusel A, et al. A human model of epithelial to mesenchymal transition to monitor drug efficacy in hepatocellular carcinoma progression. *Mol Cancer Ther*. 2011;10:850–60.
- Drake JM, Strohbehn G, Bair TB, Moreland JG, Henry MD. ZEB1 enhances transendothelial migration and represses the epithelial phenotype of prostate cancer cells. *Mol Biol Cell*. 2009;20:2207–17.
- Leshem O, Madar S, Kogan-Sakin I, Kamer I, Goldstein I, Brosh R, et al. TMPRSS2/ERG promotes epithelial to mesenchymal transition through the ZEB1/ZEB2 axis in a prostate cancer model. *PLoS One*. 2011;6:e21650.
- Kong D, Banerjee S, Ahmad A, Li Y, Wang Z, Sethi S, et al. Epithelial to mesenchymal transition is mechanistically linked with stem cell signatures in prostate cancer cells. *PLoS One*. 2010;5:e12445.
- Roca H, Hernandez J, Weidner S, McEachin RC, Fuller D, Sud S, et al. Transcription factors OVOL1 and OVOL2 induce the Mesenchymal to epithelial transition in human cancer. *PLoS One*. 2013;8:e76773.
- Takahashi E, Nagano O, Ishimoto T, Yae T, Suzuki Y, Shinoda T, et al. Tumor necrosis factor-α regulates transforming growth factor-β-dependent epithelial-Mesenchymal transition by promoting Hyaluronan-CD44-Moesin interaction. *J Biol Chem*. 2010;285:4060–73.
- Edgar R, Domrachev M, Lash AE. Gene expression Omnibus: NCBI gene expression and hybridization array data repository. *Nucleic Acids Res*. 2002;30:207–10.
- Rung J, Brazma A. Reuse of public genome-wide gene expression data. *Nat Rev Genet*. 2012;14:1–11.
- Pierre M, DeHertogh B, Gaigneaux A, DeMeulder B, Berger F, Bareke E, et al. Meta-analysis of archived DNA microarrays identifies genes regulated by hypoxia and involved in a metastatic phenotype in cancer cells. *BMC Cancer*. 2010;10:176.
- Sontrop HJM, Verhaegh WFJ, Reinders MJT, Moerland PD. An evaluation protocol for subtype-specific breast cancer event prediction. *PLoS One*. 2011;6:e21681.
- Chen M, Wang K, Zhang L, Li C, Yang Y. The discovery of putative urine markers for the specific detection of prostate tumor by integrative mining of public genomic profiles. *PLoS One*. 2011;6:e28552.
- Gröger CJ, Grubinger M, Waldhör T, Vierlinger K, Mikulits W. Meta-analysis of Gene expression signatures defining the epithelial to Mesenchymal transition during cancer progression. *PLoS One*. 2012;7:e51136.
- Button KS, Ioannidis JP a, Mokrysz C, Nosek B a, Flint J, Robinson ESJ, et al. power failure: why small sample size undermines the reliability of neuroscience. *Nat. Rev. Neurosci*. 2013;14:365–76.
- Zöllner S, Pritchard JK. Overcoming the Winner's curse: estimating penetrance parameters from case-control data. *Am J Hum Genet*. 2007;80:605–15.
- Choi JK, Yu U, Kim S, Yoo OJ. Combining multiple microarray studies and modeling interstudy variation. *Bioinformatics*. 2003;19:i84–90.
- Eklund AC, Szallasi Z. Correction of technical bias in clinical microarray data improves concordance with known biological information. *Genome Biol*. 2008;9:R26.
- Leek JT. Svsseq: removing batch effects and other unwanted noise from sequencing data. *Nucleic Acids Res*. 2014;42:e161.
- Bolstad BM, Irizarry RA, Åstrand M, Speed TP. A comparison of normalization methods for high density oligonucleotide array data based on variance and bias. *Bioinformatics*. 2003;19:185–93.
- Leek JT, Storey JD. Capturing heterogeneity in gene expression studies by surrogate variable analysis. *PLoS Genet*. 2007;3:1724–35.
- Shabalin AA, Tjelmeland H, Fan C, Perou CM, Nobel AB. Merging two gene-expression studies via cross-platform normalization. *Bioinformatics*. 2008;24: 1154–60.
- Baker FB, Hubert LJ. Measuring the power of hierarchical cluster analysis. *J Am Stat Assoc*. 1975;70:31–8.
- Langfelder P, Horvath S. WGCNA: an R package for weighted correlation network analysis. *BMC Bioinformatics*. 2008;9:559.
- Rhodes DR, Yu J, Shanker K, Deshpande N, Varambally R, Ghosh D, et al. ONCOMINE: a cancer microarray database and integrated data-mining platform. *Neoplasia*. 2004;6:1–6.
- Smith JJ, Deane NG, Wu F, Merchant NB, Zhang B, Jiang A, et al. Experimentally derived metastasis Gene expression profile predicts recurrence and death in patients with Colon cancer. *Gastroenterology*. 2010;138:958–68.
- Schmidt M, Böhm D, Von Törne C, Steiner E, Puhl A, Pilch H, et al. The humoral immune system has a key prognostic impact in node-negative breast cancer. *Cancer Res*. 2008;68:5405–13.
- Hatzis C, Pusztai L, Valero V, Booser DJ, Esserman L, Lluch A, et al. A Genomic Predictor of Response and Survival Following Taxane-Anthracycline



- Chemotherapy for Invasive Breast Cancer. *JAMA J. Am. Med. Assoc.* 2011;305:1873–1881.
42. Glück S, Ross JS, Royce M, McKenna EF, Perou CM, Avisar E, et al. TP53 genomics predict higher clinical and pathologic tumor response in operable early-stage breast cancer treated with docetaxel-capecitabine ?? Trastuzumab Breast Cancer Res Treat. 2012;132:781–91.
  43. Desmedt C, Piette F, Loi S, Wang Y, Lallemand F, Haibe-Kains B, et al. Strong time dependence of the 76-gene prognostic signature for node-negative breast cancer patients in the TRANSBIG multicenter independent validation series. *Clin Cancer Res.* 2007;13:3207–14.
  44. Director's Challenge Consortium for the Molecular Classification of Lung Adenocarcinoma K, Shedden K, Taylor JMG, Enkemann SA, Tsao M-S, Yeatman TJ, et al. Gene expression-based survival prediction in lung adenocarcinoma: a multi-site, blinded validation study. *Nat. Med.* 2008;14:822–7.
  45. Okayama H, Kohno T, Ishii Y, Shimada Y, Shiraishi K, Iwakawa R, et al. Identification of genes upregulated in ALK-positive and EGFR/KRAS/ALK-negative lung adenocarcinomas. *Cancer Res.* 2012;72:100–11.
  46. Taylor BS, Schultz N, Hieronymus H, Gopalan A, Xiao Y, Carver BS, et al. Integrative genomic profiling of human prostate cancer. *Cancer Cell.* 2010;18:11–22.
  47. Sean D, Meltzer PS. GEOquery: a bridge between the Gene expression Omnibus (GEO) and BioConductor. *Bioinformatics.* 2007;23:1846–7.
  48. Grimmett GR. On the number of clusters in the percolation model. *J. London Math. Soc.* 1976. p. 346–50.
  49. Subramanian A, Tamayo P, Mootha VK, Mukherjee S, Ebert BL, Gillette MA, et al. Gene set enrichment analysis: a knowledge-based approach for interpreting genome-wide expression profiles. *Proc Natl Acad Sci.* 2005;102:15545–50.
  50. Coradini D, Boracchi P, Ambrogi F, Biganzoli E, Oriana S. Cell polarity, epithelial-mesenchymal transition, and cell-fate decision gene expression in ductal carcinoma in situ. *Int J Surg Oncol.* 2012;2012
  51. Moreno-Bueno G, Portillo F, Cano a. Transcriptional regulation of cell polarity in EMT and cancer. *Oncogene.* 2008;27:6958–69.
  52. Lamouille S, Xu J, Derynck R. Molecular mechanisms of epithelial–mesenchymal transition. *Nat Rev Mol Cell Biol.* 2014;15:178–96.
  53. Newkirk KM, Parent AE, Fossey SL, Choi C, Chandler HL, Rajala-Schultz PJ, et al. Snai2 {expression} {enhances} {ultraviolet} {radiation}-{induced} {skin} {carcinogenesis}. *Am J Pathol.* 2007;171:1629–39.
  54. Hudson LG, Choi C, Newkirk KM, Parkhani J, Cooper KL, Lu P, et al. Ultraviolet radiation stimulates expression of snail family transcription factors in keratinocytes. *Mol Carcinog.* 2007;46:257–68.
  55. Shao DD, Xue W, Krall EB, Bhutkar A, Piccioni F, Wang X, et al. KRAS and YAP1 converge to regulate EMT and tumor survival. *Cell.* 2014;158:171–84.
  56. Goswami MT, Reka AK, Kurapati H, Kaza V, Chen J, Standiford TJ, et al. Regulation of complement-dependent cytotoxicity by TGF- $\beta$ -induced epithelial-mesenchymal transition. *Oncogene.* 2016;35:1888–98.
  57. Yokoyama S, Asahara H. The myogenic transcriptional network. *Cell Mol Life Sci.* 2011;68:1843–9.
  58. Higgins DF, Kimura K, Bernhardt WM, Shrimanker N, Akai Y, Hohenstein B, et al. Hypoxia promotes fibrogenesis in vivo via HIF-1 stimulation of epithelial-to-mesenchymal transition. *J Clin Invest.* 2007;117:3810–20.
  59. Reaves DK, Fagan-Solis KD, Dunphy K, Oliver SD, Scott DW, Fleming JM. The role of lipolysis stimulated lipoprotein receptor in breast cancer and directing breast cancer cell behavior. Fanning AS, editor. *PLoS One.* 2014;9:e91747.
  60. Wang X, Yang J, Qian J, Liu Z, Chen H, Cui Z. S100A14, a mediator of epithelial-mesenchymal transition, regulates proliferation, migration and invasion of human cervical cancer cells. *Am J Cancer Res.* 2015;5:1484–95.
  61. Xu X, Su B, Xie C, Wei S, Zhou Y, Liu H, et al. Sonic hedgehog-Gli1 signaling pathway regulates the epithelial Mesenchymal transition (EMT) by mediating a new target gene, S100A4, in pancreatic cancer cells. *PLoS One.* 2014;9:e96441.
  62. Kawahara T, Hotta N, Ozawa Y, Kato S, Kano K, Yokoyama Y, et al. Quantitative proteomic profiling identifies DPYSL3 as pancreatic ductal adenocarcinoma-associated molecule that regulates cell adhesion and migration by stabilization of focal adhesion complex. *PLoS One.* 2013;8:e79654.
  63. Kanda M, Nomoto S, Oya H, Shimizu D, Takami H, Hibino S, et al. Dihydropyrimidinase-like 3 facilitates malignant behavior of gastric cancer. *J Exp Clin cancer Res CR.* 2014;33:66.
  64. Li Y, Zeng Y, Mooney SM, Yin B, Mizokami A, Namiki M, et al. Resistance to paclitaxel increases the sensitivity to other microenvironmental stresses in prostate cancer cells. *J Cell Biochem.* 2011;112:2125–37.
  65. Steketeer K, Ziel-van der Made ACJ, van der Korput HAGM, Houstmuller AB, Trapman J A bioinformatics-based functional analysis shows that the specifically androgen-regulated gene SARG contains an active direct repeat androgen response element in the first intron *J Mol Endocrinol.* 2004;33:477–91.
  66. Vu T, Jin L, Datta P. Effect of Cigarette Smoking on Epithelial to Mesenchymal Transition (EMT) in Lung Cancer. *J. Clin. Med. Multidisciplinary Digital Publishing Institute.* 2016;5:44.
  67. Milara J, Peiro T, Serrano A, Cortijo J. Epithelial to mesenchymal transition is increased in patients with COPD and induced by cigarette smoke. *Thorax BMJ Publishing Group Ltd.* 2013;68:410–20.
  68. Nagathihalli NS, Massion PP, Gonzalez AL, Lu P, Datta PK. Smoking induces epithelial-to-Mesenchymal transition in non-small cell lung cancer through HDAC-mediated Downregulation of E-cadherin. *Mol Cancer Ther.* 2012;11:2362–72.
  69. Fischer KR, Durrans A, Lee S, Sheng J, Li F, Wong STC, et al. Epithelial-to-mesenchymal transition is not required for lung metastasis but contributes to chemoresistance. *Nature Nature Research.* 2015;527:472–6.
  70. Zheng X, Carstens JL, Kim J, Scheible M, Kaye J, Sugimoto H, et al. Epithelial-to-mesenchymal transition is dispensable for metastasis but induces chemoresistance in pancreatic cancer. *Nature Nature Publishing Group.* 2015;527:525–30.
  71. McKiernan E, McDermott EW, Evoy D, Crown J, Duffy MJ. The role of S100 genes in breast cancer progression. *Tumor Biol.* 2011;32:441–50.
  72. Mak P, Leav I, Pursell B, Bae D, Yang X, Taglienti CA, et al. ERbeta impedes prostate cancer EMT by destabilizing HIF-1alpha and inhibiting VEGF-mediated snail nuclear localization: implications for Gleason grading. *Cancer Cell NIH Public Access.* 2010;17:319–32.
  73. Liberzon A, Birger C, Thorvaldsd??Ttir H, Ghandi M, Mesirov JP, Tamayo P. The molecular signatures database Hallmark Gene set collection. *Cell Syst.* 2015;1:417–25.

Submit your next manuscript to BioMed Central and we will help you at every step:

- We accept pre-submission inquiries
- Our selector tool helps you to find the most relevant journal
- We provide round the clock customer support
- Convenient online submission
- Thorough peer review
- Inclusion in PubMed and all major indexing services
- Maximum visibility for your research

Submit your manuscript at  
www.biomedcentral.com/submit

